JOURNAL OF Materials CHEMISTRY

Structural and Mössbauer study of Sr_2FeO_3X (X = F, Cl, Br) and the magnetic structure of Sr_2FeO_3F

Andrew L. Hector,[a] John A. Hutchings,[b] Richard L. Needs,[a] Michael F. Thomas[b] and Mark T. Weller*[a]

[a]*Department of Chemistry, University of Southampton, Highfield, Southampton, UK SO17 1BJ*
[b]*Department of Physics, University of Liverpool, Oxford Street, Liverpool, UK L69 7ZE. E-mail: mtw@soton.ac.uk*

Received 16th October 2000, Accepted 30th October 2000
First published as an Advance Article on the web 19th December 2000

The structures of Sr_2FeO_3F, Sr_2FeO_3Cl and Sr_2FeO_3Br have been investigated using powder neutron diffraction (PND). All three ferrates crystallise in the primitive tetragonal space group *P*4/*nmm* and the anions are fully ordered giving iron oxygen square pyramids separated by rock salt type layers of strontium halide. ^{57}Fe Mössbauer data have been collected and confirm one iron(III) site of distorted octahedral geometry in all three structures. Variable temperature PND data have been used to determine the $\sqrt{2}a \times 2c$ magnetic superstructure of Sr_2FeO_3F.

Introduction

Layered complex oxides of the transition metals have been the subject of intensive research for many years due to the wide variety of electronic and magnetic properties which they exhibit. The method of choice for control of the transition metal oxidation state has normally been to vary the A-type site cation, for example replacement of La^{3+} with Ba^{2+} in $La_{2-x}Ba_xCuO_4$ produces a copper oxidation state of $2+x$.[1] Alternatively another metal can be doped onto the B-type site, as in the copper(III) containing $La_2Cu_{0.5}Li_{0.5}O_4$.[2] The recent discovery of superconductivity in the K_2NiF_4-type structure $Sr_2CuO_2F_{2+\delta}$[3] has prompted a high level of interest in the use of a mixture of anions as a tool for oxidation state control.

A number of iron(III) oxides which adopt the K_2NiF_4-type structure are known, with the composition $ALnFeO_4$ (A = Ca,[4] Sr[5,6] or Ba;[7] Ln = lanthanide). All crystallise with regular *I*4/*mmm* tetragonal structures with FeO_6 octahedra slightly elongated along the *c*-axis. The magnetic structures of $CaLaFeO_4$[4] and $SrLaFeO_4$[5] are characterised by antiferromagnetic interactions between nearest-neighbour Fe^{3+} sites. This was observed by powder neutron diffraction (PND) as a $\sqrt{2}a \times c$ magnetic superstructure cell and has been described by the use of an orthorhombic (*Cmca*) space group. The ordering is purely two-dimensional and no magnetic interaction between the layers is observed.

The phases Sr_2FeO_3F and K_2NbO_3F were initially reported by Galasso and Darby[8] as containing oxide and fluoride statistically distributed about the apical sites of the transition metal co-ordination octahedra. However, a later investigation of the structure of Sr_2FeO_3F reported that, although the previous structure was basically correct, there were weak reflections in the X-ray diffraction pattern which could not be indexed on the suggested body centred tetragonal lattice.[9] Recent work by ourselves has demonstrated that the body-centred *I*4/*mmm* structure, with a mixture of oxide and fluoride on the apical sites of the B-cation octahedra, does accurately describe the structures of Ba_2ScO_3F[10] and K_2NbO_3F.[11] Ba_2InO_3F[10] and Sr_2FeO_3F[11] have, however, been demonstrated to have segregated oxide and fluoride layers, resulting in a primitive *P*4/*nmm* cell and effective square pyramidal MO_5 co-ordination of the B-cation. Some high *d*-spacing reflections in the PND pattern of Sr_2FeO_3F were still unassigned and were believed to be associated with long range magnetic order of the Fe^{3+} ions.

The magnetic susceptibility of Sr_2FeO_3F has been measured from 4.2 to 650 K.[9] A smooth minimum was observed in the susceptibility centred at around 480 K, which was taken as an indication of two-dimensional antiferromagnetism. In the same work Mössbauer spectra were recorded; iron(III) was observed at 363 K which is fully magnetically ordered at 4.2 K. The Néel temperature was derived as 358 K. At room temperature the spectrum was found to be a broadened sextet which was attributed to relaxation effects close to T_N.

Sr_2FeO_3Cl and Sr_2FeO_3Br have been reported by Ackerman.[12] Lattice parameters were listed for these and a number of related phases. They were stated to be isostructural with Ca_2FeO_3Cl, for which a single crystal X-ray diffraction structure was determined. No systematic absences were observed and the structure was described using the space group *P*4, however the structure reported was virtually identical to that of Sr_2FeO_3F.

In this paper we report the nuclear and magnetic structures of Sr_2FeO_3F at 2.4, 293 and 390 K by PND. The ambient temperature structures of Sr_2FeO_3Cl and Sr_2FeO_3Br have been determined using this technique. ^{57}Fe Mössbauer spectra of Sr_2FeO_3F, Sr_2FeO_3Cl and Sr_2FeO_3Br at 4.2, 293 and 390 K have been collected and will be discussed with respect to the crystal structures.

Experimental

Red-brown samples of Sr_2FeO_3X (X = Cl, Br) were prepared by firing a 1 : 3 : 1 mixture of Fe_2O_3 (BDH, 99.95%), $SrCO_3$ (Aldrich, 98%) and SrX_2 ($SrCl_2 \cdot 6H_2O$, Hogg Laboratory Supplies; $SrBr_2$, Strem, 99%) in air at 850 °C for 4 days, reground after 1 day. The same method with strontium fluoride, even under flowing argon or nitrogen, resulted in black, oxidised products. This was overcome by heating Fe_2O_3 (dried at 200 °C), SrO (from $SrCO_3$ at 1000 °C) and SrF_2 (Aldrich, 99.99%, dried at 200 °C) at 900 °C in an alumina crucible sealed under vacuum into a silica ampoule.

Samples were initially assessed by powder X-ray diffraction,

DOI: 10.1039/b008321f

data were collected using a Siemens D5000 diffractometer employing Cu $K_{\alpha 1}$ radiation ($\lambda = 1.5406$ Å) over the 2θ range 20–120°. Powder neutron diffraction data were collected for Sr_2FeO_3F and Sr_2FeO_3Cl on Polaris, the medium resolution diffractometer at the ISIS facility, for 2–3 hours. For the purposes of structural refinement, the high resolution ($\Delta d/d = 5 \times 10^{-3}$) backscattered detector (C) bank was used. For magnetic structures the lower resolution ($\Delta d/d = 1 \times 10^{-2}$) low angle (A) bank was also used, with the advantage of a higher *d*-spacing range, to ~9 Å, where the magnetic reflections are most significant. Data for Sr_2FeO_3Br were collected for 6 hours on the D2B high resolution constant wavelength diffractometer at the Institute Laue-Langevin. Neutrons of wavelength 1.594 Å were selected, for structural refinement data in the range 20–160° were used.

Rietveld refinements were carried out using the GSAS package,[13] neutron scattering lengths and absorption cross sections were taken from Köster *et al.*[14] Initially the lattice parameters, background, peak shape and neutron absorption were refined. Atom positions and temperature factors were then introduced. Magnetic refinements used a calculated iron magnetic form factor.[15]

Mössbauer spectra were collected at 4.2, 293 and 390 K in order to investigate the magnetic properties of all three iron oxide halides at the diffraction data collection temperature and both well above and below the antiferromagnetic ordering temperature. The data were collected using a standard Mössbauer spectrometer at the Oliver Lodge Laboratory, Liverpool University with all quoted chemical shifts referenced to α iron at 300 K. The data analyses reported below were derived by computer modelling of spectra calculated by Kundig.[16]

Thermogravimetric analysis was carried out with a Polymer Laboratories STA1500 under a stream of 5%H_2/N_2. Slightly oxidised samples of $Sr_2FeO_{3.1}F_{0.9}$ prepared under argon, as previously reported by Menil *et al.*,[9] showed a weight loss at 825 °C consistent with reduction of $Fe^{3.1+}$ to Fe^{3+}. This weight loss was not observed in the samples investigated in this work indicating that no oxidation of the iron site had occurred.

Results and discussion

Structure determination of Sr_2FeO_3Cl and Sr_2FeO_3Br

Initially the Sr_2FeO_3Br structure was refined using the *P*4 model described by Ackerman for Ca_2FeO_3Cl.[12] Refinement of atom positions and temperature factors introduced a degree of instability, but this could be overcome by strongly damping the movement of these parameters. Inspection of the refined positional parameters from this model showed them to be essentially the same as those in a structure description using the higher symmetry space group *P*4/*nmm* of Ba_2InO_3F[10] and Sr_2FeO_3F[11] and so this model was input and used thereafter. Refinement of the ambient temperature structures of Sr_2FeO_3Cl and Sr_2FeO_3Br in space group *P*4/*nmm* proceeded smoothly and was more stable than using the *P*4 model. Fig. 1 shows the final fit obtained with Sr_2FeO_3Br and Table 1 gives the refined crystallographic data for both phases. The bond lengths and temperature factors finally obtained (listed later with those of the fluoride in Table 4) were very similar to those obtained in *P*4, except that it was possible to refine anisotropic temperature factors in the higher symmetry model without introducing instability. The structure of Sr_2FeO_3Cl is represented graphically in Fig. 2.

The lattice parameters obtained in this work are considerably different from those obtained in the single crystal study.[12] The *a*-axis (Cl 3.96 Å, Br 3.97 Å) was similar but the *c*-axis (Cl 13.98 Å, Br 15.04 Å) was considerably shorter than in this work. The synthesis methods used were very different, the single crystals being grown from a melt of the appropriate strontium halide. No strontium oxide or carbonate was added and partial, uncontrolled hydrolysis was relied upon as a source of oxide. Hence it is likely that some non-stoichiometry was present in the single crystals, although the colour indicates that the iron was still present as Fe^{3+}.

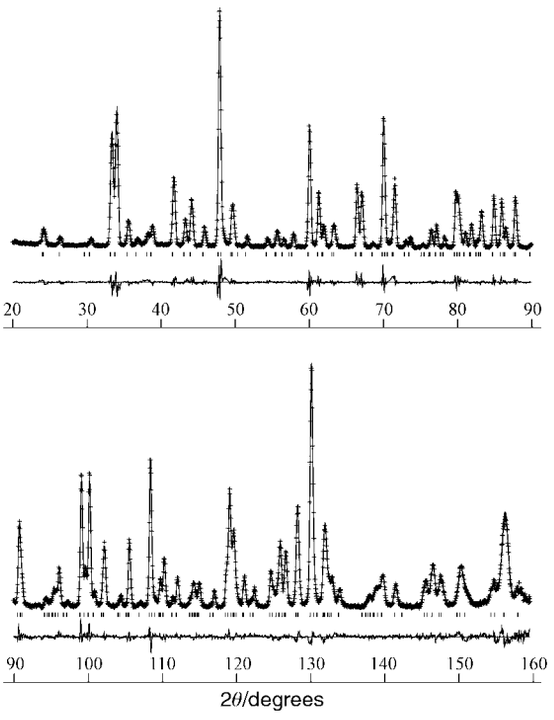

Fig. 1 Final fit to the PND pattern of Sr_2FeO_3Br. Data points are marked as crosses, profile fit as the upper continuous line and difference as the lower continuous line.

Table 1 Refined crystallographic parameters for Sr_2FeO_3X (X = Cl, Br)

		Sr_2FeO_3Cl		Sr_2FeO_3Br	
Atom	Site	*z*	U_{eq}/Å^2	*z*	U_{eq}/Å^2
Fe	¾, ¾, *z* (2c)	0.20748(4)	0.50(2)	0.19566(9)	0.63(8)
Sr(1)	¼, ¼, *z* (2c)	0.09641(6)	0.80(3)	0.0910(1)	0.82(9)
Sr(2)	¼, ¼, *z* (2c)	0.34513(5)	0.71(4)	0.3252(1)	1.00(6)
O_{ba}	¾, ¼, *z* (4f)	0.23115(4)	0.72(3)	0.21771(9)	0.81(9)
O_{ax}	¾, ¾, *z* (2c)	0.07533(7)	1.10(3)	0.0707(1)	1.05(6)
X	¾, ¾, *z* (2c)	0.42522(5)	1.07(3)	0.4158(1)	1.96(8)

*P*4/*nmm*; Sr_2FeO_3Cl $a = 3.9239(1)$ Å, $c = 14.2976(5)$ Å, $R_{wp} = 1.64\%$, $R_p = 2.04\%$; Sr_2FeO_3Br $a = 3.9307(1)$ Å, $c = 15.1516(6)$ Å, $R_{wp} = 4.87\%$, $R_p = 6.33\%$. O_{ba} and O_{ax} are in basal and equatorial positions, respectively, in the FeO_5 square pyramids.

^{57}Fe Mössbauer spectroscopy

^{57}Fe Mössbauer spectra were collected for all three samples at 4.2, 293 and 390 K. Selected spectra are shown in Figs. 3 and 4 and the parameters used to fit the spectra are summarised in Table 2.

The 4.2 K ^{57}Fe Mössbauer spectra of Sr_2FeO_3F, Sr_2FeO_3Cl and Sr_2FeO_3Br are all practically identical and can be fitted by a single sextet. The values of the chemical isomer shift (δ) and the hyperfine field (B_{hf}) are consistent with iron present solely as Fe^{3+}.[17] The single sextet spectra show all iron atoms are in one environment and their magnetic moments make the same angle (θ) to the principle axis of the electric field gradient (V_{zz}), which is expected to be along the *z*-axis. The spectra also show there is no iron containing impurity present in any of the samples. Comparing between the different halides shows only

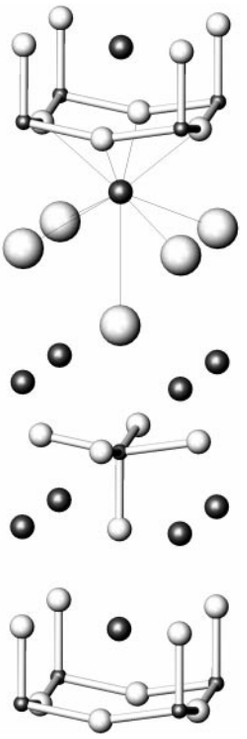

Fig. 2 Structure of Sr_2FeO_3Cl showing FeO_5 square pyramids and the SrO_4F_5 co-ordination sphere.

small differences in the spectra, as is expected from their high degree of structural similarity. Sr_2FeO_3F has slightly smaller values of δ and B_{hf} indicating a less localised iron 3d shell, showing that these iron atoms are more covalently bound to the oxygen ions than in Sr_2FeO_3Cl or Sr_2FeO_3Br. The magnitude of the quadrupole splitting at $T > T_N$ varies according to $|\Delta_F| > |\Delta_{Cl}| > |\Delta_{Br}|$. For $T < T_N$ the resultant

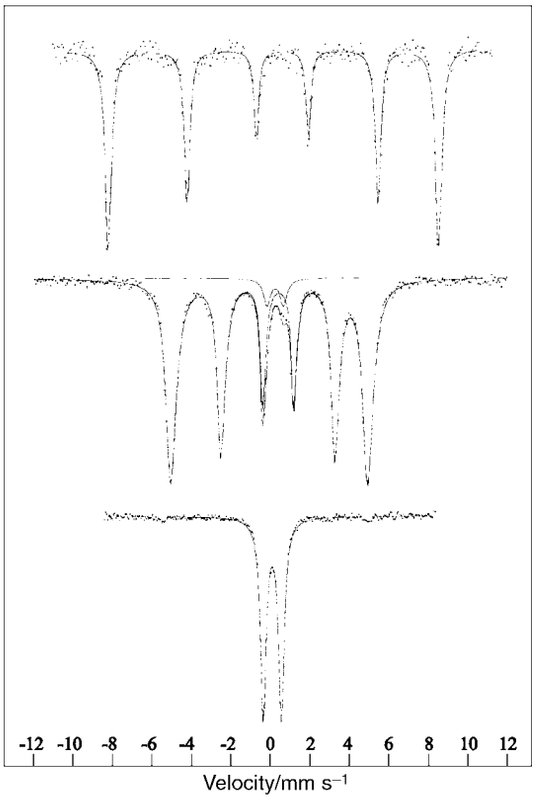

Fig. 3 ^{57}Fe Mössbauer spectra of Sr_2FeO_3F at 4.2 (top), 293 (middle) and 390 K (bottom).

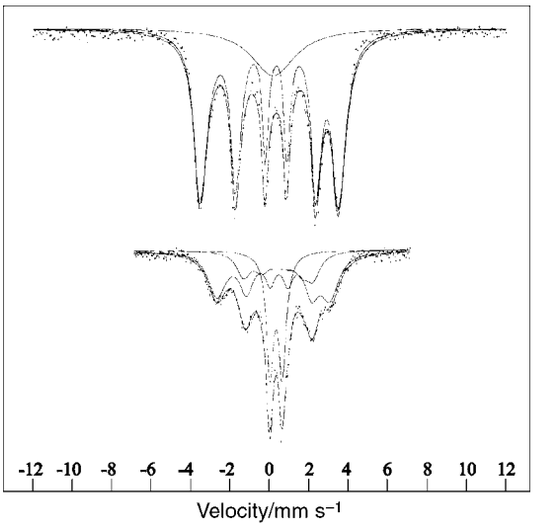

Fig. 4 ^{57}Fe Mössbauer spectra of Sr_2FeO_3Cl (top) and Sr_2FeO_3Br (bottom) at 293 K.

quadrupole interaction, the quadrupole shift, is given by the expression:[18]

$$\Delta \propto V_{zz}(3\cos^2\theta - 1)$$

From the 4.2 K data alone it is not clear whether these differences arise from differing V_{zz} or θ values or both.

Spectra collected at 390 K are very similar for all three phases and consist of a doublet with chemical isomer shift, δ, appropriate to Fe^{3+}. The doublet indicates that at this temperature there is no magnetic order. As observed at 4.2 K, Δ is larger in Sr_2FeO_3F than either Sr_2FeO_3Cl or Sr_2FeO_3Br, which are both very similar.

The Mössbauer spectra collected at 293 K are considerably less alike for the three oxide halides. Compared with the 4.2 K data there is a sharp reduction in B_{hf}. The Néel temperature (T_N) is being approached and fluctuations of the magnetic moment reduce the hyperfine field. The reduction in B_{hf} is most and least pronounced in Sr_2FeO_3Br and Sr_2FeO_3F respectively, from this $T_N(F) > T_N(Cl) > T_N(Br)$. Further evidence for this order of ascending T_N is the appearance of absorption near the centre of the spectra, corresponding to iron atoms experiencing a fast fluctuating or zero hyperfine field, which is greatest in Sr_2FeO_3Br and least in Sr_2FeO_3F.

The variation in chemical isomer shift with temperature for all three phases is consistent with a second order Doppler effect,[19] no change in charge state of the iron is observed on heating. The value of the quadrupole splitting, Δ, is very similar at each data collection temperature for both Sr_2FeO_3Cl and Sr_2FeO_3Br, but significantly larger for Sr_2FeO_3F. The iron–oxygen–halogen co-ordination octahedra have been shown as highly asymmetrical from the refinement of diffraction data and may be considered as a square based pyramid of oxide. In Sr_2FeO_4,[20] with a similar structure but based on Fe^{4+} and a reasonably regular charge distribution about the iron centre, the quadrupole splitting is reported as -0.33 mm s^{-1} at 4.2 K, clearly more equivalent to those of the oxide chlorides and bromides. The most obvious difference between the iron co-ordination environments of these two phases and their fluoride analogue is the presence of the small highly electronegative F^- anion. The asymmetry of the iron centre electron distribution is affected differently as both chloride and bromide are of similar electronegativity to oxide but fluoride is substantially more electronegative and creates a bigger charge asymmetry and consequently a greater quadrupole splitting.

The negative sign of Δ is seen by lines 1 and 2 being more split than 5 and 6, numbering the lines from negative to positive δ. A negative quadrupole splitting, as found in all spectra

Table 2 Refined Mössbauer parameters for the iron oxide halides

	Sr_2FeO_3F			Sr_2FeO_3Cl			Sr_2FeO_3Br		
T/K	δ/mm s^{-1}	Δ/mm s^{-1}	B_{hf}/kG	δ/mm s^{-1}	Δ/mm s^{-1}	B_{hf}/kG	δ/mm s^{-1}	Δ/mm s^{-1}	B_{hf}/kG
4.2	0.39	−0.47	520	0.41	−0.34	522	0.41	−0.33	523
293	0.29	−0.44	311	0.31	−0.32	219	0.32	−0.30	182
390	0.24	0.93	0	0.26	0.67	0	0.26	0.64	0

The errors in the chemical isomer shift, δ, and the quadrupolar splitting, Δ, are ± 0.01 mm s^{-1}, and ± 1 kG in the hyperfine field, B_{hf}.

recorded at 4.2 and 293 K, is normally produced by an excess of electrons concentrated along the polar (z) axis with respect to the equatorial (xy) plane. The increase in V_{zz} from Sr_2FeO_3F through to Sr_2FeO_3Br may be connected to differences in the geometry and anion type changing the electric field gradient of the iron nucleus.[18] However such changes in co-ordination can also polarise the closed shells of electrons about the nucleus which may alter the charge symmetry seen by the nucleus *i.e.* there may be a deviation away from the totally symmetric ground state.

With no magnetic order at 390 K the magnitude, although not the sign, of the quadrupole splitting in Sr_2FeO_3F is given by:

$$\Delta_{390} = \left| \tfrac{1}{2} eQV_{zz} \right| = 0.93 \text{ mm s}^{-1}$$

(e = proton charge, Q = nuclear quadrupole moment).

Below T_N, at 4.2 and 293 K, the main line splitting is caused by magnetic dipole interaction. The quadrupole shift, the projection of the quadrupole interaction on the magnetic dipole axis, is treated as a perturbation and may be represented as:

$$\Delta = \tfrac{1}{2} eQV_{zz} \cdot \tfrac{1}{2}(3\cos^2\theta - 1)$$

where θ is the angle between V_{zz} and the magnetic axis. At 4.2 K the values measured for Sr_2FeO_3F are:

$$(-0.47 \pm 0.01) = (\pm 0.93 \pm 0.01) \cdot \tfrac{1}{2}(3\cos^2\theta - 1)$$

which give alternative values of $\theta = 87 \pm 15^\circ$ or $\theta = 35 \pm 2^\circ$ corresponding to positive or negative signs for $\frac{1}{2}eQV_{zz}$. This is consistent with the result of Menil *et al.*[9] The assumption, from symmetry, that V_{zz} is aligned along the c axis favours the solution $\theta \sim 90^\circ$ with the magnetic moment lying in the ab plane and a positive sign for $\frac{1}{2}eQV_{zz}$.

In K_2NiF_4 structures there is pseudo two dimensional magnetic ordering, the strongest interactions being in the Fe–O plane. In general a higher T_N is associated with simple oxide linkages, as this gives the most effective superexchange mechanism. In these structures the shortest Fe–O basal distances are in Sr_2FeO_3F, implying that this phase will have the highest T_N. The Fe–O–Fe angle in these planes should also be as near to 180° as possible for the most effective superexchange, the largest deviation occurs in Sr_2FeO_3F (159.8°) and the smallest in Sr_2FeO_3Br (160.7°). The difference in this angle between all three phases is small, $<1^\circ$, so this change would be expected to only slightly change the degree of superexchange. The previously reported value of T_N for the oxide fluoride is 358 K, in agreement with the observation from this study that $273 \text{ K} < T_N < 390$ K. The superexchange mechanism is generally considered most efficient through short oxide bonds and would not be expected to lead to a high degree of magnetic interaction between the planes.

Nuclear and magnetic structure determination of Sr_2FeO_3F

The Mössbauer results and the extra high d-spacing reflections observed for Sr_2FeO_3F demonstrate the existence of long range magnetic order at room temperature and below. At room temperature Sr_2FeO_3Cl and Sr_2FeO_3Br did not exhibit extra reflections at high d-spacings. This was attributed to the higher magnetic ordering temperature in the fluoride than the chloride or bromide. To determine the magnetic structure of Sr_2FeO_3F, PND data were collected at 2, 293 and 390 K. Preliminary examination of the high d-spacing A-bank data showed that the extra reflections were strong at 2 K, weaker at 293 K and barely visible at 390 K. Hence the initial investigation utilised the 2 K data set.

All the observed reflections in the low angle PND data set were found to be indexable with a magnetic cell of dimensions $a_{mag} = \sqrt{2}a$ and $c_{mag} = 2c$. Examination of the Miller indices revealed only two systematic absences, hhl and $00l$ reflections were only observed with $l = 2n$. Three space groups have the maximum symmetry consistent with these absences and, of these, $P4_2mc$ and $P4_2/mmc$ would not allow iron positions equivalent to the nuclear cell. Hence the magnetic space group was assigned as $P\bar{4}2c$.

Initially the magnetic moment of iron was set at zero and the nuclear structure was refined. The atom positions and temperature factors were then fixed while the magnetic moment was refined as a separate magnetic phase. There are four possible arrangements of Fe^{3+} spins in $P\bar{4}2c$, as shown in Fig. 5. Initially a magnetic moment μ_x or μ_z was applied in each of these settings. The only model which attributed intensity to all the observed magnetic reflections was that with both operators set at time reversal and the moment aligned in the x-direction. Hence this model was chosen as the starting point for refinement.

In order to extract the magnetic structure, a single model to describe the nuclear and magnetic structure in $P\bar{4}2c$ was developed (refining magnetic structure as a separate phase was found to cause instability in the refinement). The A- and C-bank were jointly refined using this model with the atom positions constrained to be equivalent to the $P4/nmm$ description. The refinement was highly stable with isotropic temperature factors and achieved convergence. Anisotropic temperature factors were found to cause instability and were not used.

The refined magnetic moment was found to occur almost entirely in the xy plane (μ_x and μ_y). A small value of μ_z was obtained but the estimated standard deviation was almost as large as μ_z itself. Thus the z-axis component was fixed at 0 and $\theta = 90^\circ$, as was suggested by the Mössbauer results. It is possible that a study using an instrument better optimised for magnetic structure determination would demonstrate some

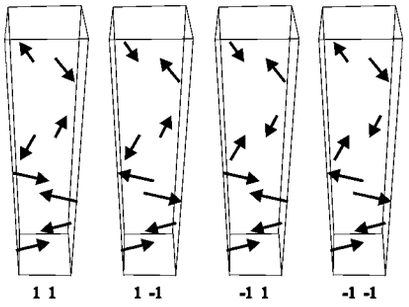

Fig. 5 Possible arrangements of the Fe^{3+} spins in $P\bar{4}2c$ with the symmetry operators in time reversal (−1) or non-time reversal (1).

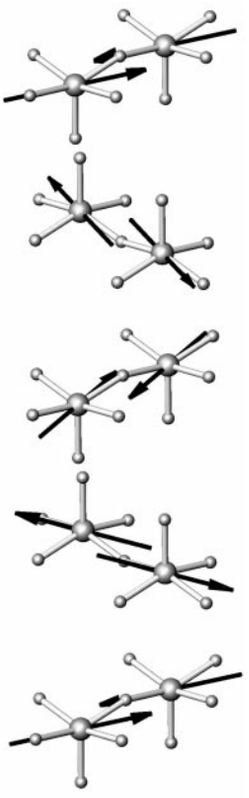

Fig. 6 Graphical representation of the magnetic supercell of Sr_2FeO_3F at 2.4 K.

canting of the spins out of the *xy* plane (as has been suggested for La_2CuO_4[21]) but none can reliably be claimed from this work.

The 2 K magnetic structure of Sr_2FeO_3F, shown in Fig. 6, shows an unusual arrangement of spins. Each layer is antiferromagnetically ordered by alternate iron spins opposing each other, not unusual for this structure type. The spins appear to align antiparallel entirely in the *xy* plane, which is more surprising since the *c*-axis doubling indicates a fairly strong interaction between layers. Some of the strongest magnetic peaks require this *c*-axis doubling. Whilst no *z*-axis component of the magnetic moment (μ_z) was demonstrable it is possible that such a component could contribute to the ordered layer stacking. The crystallographically aligned layers (*e.g.* at $z=0.11$ and $z=0.61$) have the magnetic spins aligned an angle of 18° from,

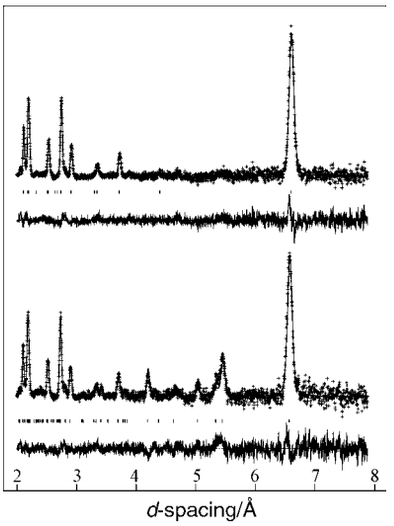

Fig. 7 Refined Polaris A-bank data for Sr_2FeO_3F at 390 (top) and 2 K (bottom) refined in *P*4/*nmm* and $P\bar{4}2c$ respectively.

alternately, the *x*- and *y*-directions. Consecutive layers linked through an Fe–O–Sr–O–Fe sequence (*e.g.* $z=0.39$ and $z=0.61$) have magnetic spins aligned normal to each other.

K_2NiF_4-type structures most often exhibit only two-dimensional magnetic ordering, where alternate iron sites in the *xy* plane have their spins opposed but the layer stacking sequence is random. This is the case in $SrLaFeO_4$[5] and Sr_2FeO_4.[20] A magnetic supercell with dimensions of $\sqrt{2}a\times 2c$ has been reported for Ca_2MnO_3[22] but the spin orientations do not appear to have been refined. A number of K_2NiF_4-type materials, such as Sr_2IrO_4,[23] have a structural ordering reminiscent of the magnetic ordering observed in Sr_2FeO_3F. The space group $I4_1/acd$ and a $\sqrt{2}a\times 2c$ cell is used to describe an arrangement of octahedral rotations (through movement of the equatorial oxygen). A similar structural distortion was applied to Sr_2FeO_3F both with and without magnetic moments included in the refinement, but this led to a worse fit to the diffraction data. Hence this possibility was discounted.

The 293 K data set was treated in a similar manner to obtain the nuclear and magnetic structure at ambient temperature. At 390 K the magnetic reflections had virtually disappeared and were not refined. A virtually identical result was obtained with the basic *P*4/*nmm* structural description and with the $P\bar{4}2c$ quadrupled cell. Fig. 7 shows the refined 2 K A-bank data set,

Table 3 Refined nuclear and magnetic structure parameters for Sr_2FeO_3F in $P\bar{4}2c$. 390 K data are presented using the magnetic supercell model for comparison, though no magnetic structure was refined

Parameter	2.4 K		293 K		390 K	
a/Å	5.45099(5)		5.46787(4)		5.48016(4)	
c/Å	26.2932(5)		26.3601(4)		26.4084(4)	
C-bank R_{wp}, R_p (%)	1.13, 1.44		3.31, 5.21		1.35, 2.42	
A-bank R_{wp}, R_p (%)	2.13, 2.73		7.02, 8.55		3.76, 4.31	
μ_x/μ_B	3.29(8)		1.6(3)		—	
μ_y/μ_B	2.00(7)		1.8(3)		—	
$\lvert\mu\rvert/\mu_B$	3.47(6)		2.38(5)		—	
ψ/°	18(1)		48(11)		—	
Atom	*z*	U_{iso}/Å^2	*z*	U_{iso}/Å^2	*z*	U_{iso}/Å^2
Fe ¼, ¼, *z* (8n)	0.11389(4)	0.29(2)	0.11381(3)	0.43(2)	0.11374(7)	0.53(3)
Sr(1) ¼, ¾, *z* (8n)	0.05247(6)	0.19(3)	0.05257(4)	0.49(2)	0.0525(1)	0.75(6)
Sr(2) ¼, ¾, *z* (8n)	0.18891(6)	0.21(3)	0.18912(4)	0.64(2)	0.1891(1)	0.69(5)
O_{ax} ¼, ¼, *z* (8n)	0.04138(9)	0.46(3)	0.04132(6)	1.03(2)	0.0418(2)	1.08(6)
F ¼, ¼, *z* (8n)	0.2168(1)	1.11(4)	0.21650(8)	2.44(4)	0.2170(2)	2.9(1)
O_{ba} 0, 0, *z* (4k); ½, ½, *z* (4l); 0, ½, *z* (4m); ½, 0, *z* (4m)	0.12667(6)	0.46(3)	0.12680(4)	0.65(2)	0.1268(1)	0.85(6)

Table 4 Derived bond lengths (Å) and angles (°) for Sr_2FeO_3F, Sr_2FeO_3Cl and Sr_2FeO_3Br at room temperature

Bond/angle	Sr_2FeO_3F	Sr_2FeO_3Cl	Sr_2FeO_3Br
$Fe–O_{ba}$	1.9633(2)	1.9908(2)	1.9936(3)
$Fe–O_{ax}$	1.912(2)	1.889(1)	1.893(2)
Fe–X	2.707(2)	3.1130(9)	3.336(4)
$O_{ax}–Fe–O_{ba}$	100.1(2)	99.7(1)	99.2(2)
$Sr(1)–O_{ba}$ ($\times 4$)	2.7507(9)	2.7494(8)	2.747(2)
$Sr(1)–O_{ax}$ ($\times 4$)	2.7500(2)	2.7909(2)	2.796(3)
$Sr(1)–O_{ax}$ ($\times 1$)	2.475(2)	2.456(1)	2.450(3)
$Sr(2)–O_{ba}$ ($\times 4$)	2.5368(8)	2.5509(6)	2.552(1)
Sr(2)–X ($\times 4$)	2.8276(6)	3.0016(4)	3.100(1)
Sr(2)–X ($\times 1$)	2.488(2)	3.283(1)	3.925(3)

O_{ax} is the oxygen in the axial site of the iron co-ordination sphere, O_{ba} is basal.

Table 5 Calculated bond valence and bond valence sum for selected atoms

Bond valence/atom sum	F	Cl	Br
$Fe–O_{ba}$	0.59	0.53	0.53
$Fe–O_{ax}$	0.67	0.70	0.70
Fe–X	0.06	0.07	0.06
Fe	3.08	2.91	2.87
O_{ba}	2.20	2.05	2.04
O_{ax}	1.80	1.75	1.74
X	0.81	1.26	1.37

contrasted with the 390 K data refined in *P4/nmm* (with no magnetic reflections). Table 3 lists the refined structure parameters.

Ambient temperature structures of Sr_2FeO_3X (X = F, Cl, Br)

The ambient temperature structures of the three phases are all very similar. The cell volume increases from Sr_2FeO_3F to Sr_2FeO_3Br, as would be expected from the ionic radii of the halides, with the biggest change from F to Cl. The change in the *a* cell parameter (3.87–3.92–3.93 Å) is small since this is mostly governed by the in-plane iron–oxygen bonding. The change in the *c* parameter (13.18–14.30–15.15 Å), which is more heavily affected by the halide, is much greater. Table 4 lists a selection of the most important bond lengths and angles. The Fe–X distance varies with the ionic radius of the halide. The O_{ba}–Fe–O_{ba} angles and the Fe–O_{ba} distance increase with the size of the halide whilst the Fe–O_{ax} distance decreases. Thus the FeO_5 square pyramid contracts in the *z*-direction and expands in the *xy* plane. The overall effect is for the pyramid volume to gradually increase across the series from 5.62 $Å^3$ (F) to 5.71 $Å^3$ (Cl) to 5.73 $Å^3$ (Br)

Bond valence calculations were carried out using the program *VaList*[24] and the results are presented in Table 5. The assignments of oxide and fluoride sites in Sr_2FeO_3F have been dealt with previously[11] and the arguments have not changed, so this will not be revisited. The first observation which should be made is that the Fe–X bond has such a low bond valence that it is effectively non-bonded. Thus the description of FeO_5 square pyramids is validated. The bond valence sum for Fe^{III} is acceptable for all three materials, although there is a general trend to lower values from F→Br for iron and oxygen, and higher value for halide. This may be due to a larger covalent contribution to the Fe–X bond with the heavier halides.

The similarity in the Mössbauer spectra of the three halides at 2.4 and 390 K, along with the structural similarity, is expected to indicate that the chloride and bromide order magnetically in the same manner as the fluoride. However the interplanar spacings increase from F to Cl to Br and it is quite possible that the magnetic ordering of Sr_2FeO_3Cl and Sr_2FeO_3Br is purely two-dimensional.

Conclusions

Sr_2FeO_3F, Sr_2FeO_3Cl and Sr_2FeO_3Br all crystallise in space group *P4/nmm*. The K_2NiF_4-type structure is modified in a manner similar to the *T** cuprates, layers of FeO_5 square based pyramids are separated by alternate layers of composition SrF and SrO. Mössbauer spectroscopy shows that only Fe^{3+} is present in all the samples from 2.4 to 390 K and that all three halides are magnetically ordered at 2.4 K. This magnetic order has been resolved in Sr_2FeO_3F by powder neutron diffraction and consists of an antiparallel alignment of alternate Fe^{3+} spins in the *xy* plane. The magnetic cell has dimensions $\sqrt{2}a \times 2c$ and may be described by space group $P\bar{4}2c$, with an unusual stacking arrangement.

Acknowledgement

This work was supported by the EPSRC under grant GR/K55578 (ALH) and through a studentship to JAH. RLN would like to thank the University of Southampton for a partial studentship. Thanks to Dr C. S. Knee (University of Southampton) for help with magnetic structure determination and to Dr R. I. Smith of the Rutherford Appleton Laboratory for assistance with neutron diffraction data collection.

References

1 J. G. Bednorz and K. A. Müller, *Z. Phys. B*, 1986, **64**, 189.
2 S. Abou-Warda, W. Pietzuch, G. Berghofer, U. Kesper, W. Massa and D. Reinen, *J. Solid State Chem.*, 1998, **138**, 18.
3 M. Al-Mamouri, P. P. Edwards, C. Greaves and M. Slaski, *Nature (London)*, 1994, **369**, 382.
4 M. M. Nguyen-Trut-Dinh, M. Vlasse, M. Perrin and G. Le Flem, *J. Solid State Chem.*, 1980, **32**, 1.
5 J. L. Soubeyroux, P. Courbin, L. Fournes, D. Fruchart and G. Le Flem, *J. Solid State Chem.*, 1980, **31**, 313.
6 J. C. Joubert, A. Collomb, D. Elmaleh, G. Le Flem, A. Daoud and G. Ollivier, *J. Solid State Chem.*, 1970, **2**, 343.
7 M. Vallino, F. Abbattista, D. Mazza and A. Delunas, *Mater. Res. Bull.*, 1986, **21**, 733.
8 F. Galasso and W. Darby, *J. Phys. Chem.*, 1962, **67**, 1451; F. Galasso and W. Darby, *J. Phys. Chem.*, 1962, **66**, 1318.
9 F. Menil, N. Kinomura, L. Fournes, J. Portier and P. Hagenmuller, *Phys. Status Solidi A*, 1981, **64**, 261; L. Fournes, N. Kinomura and F. Menil, *C. R. Acad. Sci. Paris, Ser. C*, 1980, **291**, 235.
10 R. L. Needs, M. T. Weller, U. Scheler and R. K. Harris, *J. Mater. Chem.*, 1996, **6**, 1219.
11 G. S. Case, A. L. Hector, W. Levason, R. L. Needs, M. F. Thomas and M. T. Weller, *J. Mater. Chem.*, 1999, **9**, 2821.
12 J. F. Ackerman, *J. Solid State Chem.*, 1991, **92**, 496.
13 C. Larson and R. B. Von Dreele, *GSAS, Generalised Structure Analysis System*, MS-H805, Los Alamos, NM, 1990.
14 L. Köster, H. Rauch and E. Seymann, *At. Data Nucl. Data Tables*, 1991, **49**, 65.
15 P. J. Brown, in *International Tables for Crystallography*, T. Hahn (Ed.), vol. C, Kluwer Academic Publishers, Dordrecht, 1992.
16 W. Kundig, *Nucl. Instrum. Methods*, 1967, **48**, 219.
17 F. Menil, *J. Phys. Chem. Solids*, 1985, **46**, 763.
18 N. N. Greenwood and T. C. Gibb, *Mössbauer Spectroscopy*, Chapman and Hall, London, 1971.
19 G. K. Shenoy and F. E. Wagner, *Mössbauer Isomer Shifts*, North-Holland, Amsterdam, 1978.
20 S. E. Dann, M. T. Weller, D. B. Currie, M. F. Thomas and A. D. Al-Rawwas, *J. Mater. Chem.*, 1993, **3**, 1231.
21 T. Thio, T. R. Thurston, N. W. Preyer, P. J. Picone, M. A. Kastner, H. P. Jenssen, D. R. Gabbe, C. Y. Chen, R. J. Birgeneau and A. Aharony, *Phys. Rev. B: Solid State*, 1988, **38**, 905.
22 D. E. Cox, G. Shirane, R. J. Birgeneau and J. B. MacChesney, *Phys. Rev.*, 1969, **188**, 930.
23 Q. Huang, J. L. Soubeyroux, O. Chmaissem, I. N. Sora, A. Santoro, R. J. Cava, J. J. Krajewski and W. F. Peck, Jr., *J. Solid State Chem.*, 1994, **112**, 355.
24 *VaList* computer program, A. S. Wills and I. D. Brown, CEA, France, 1999. Bond valence parameters from: I. D. Brown and D. Altermatt, *Acta Crystallogr., Sect. B*, 1985, **41**, 244; N. E. Brese and M. O'Keeffe, *Acta Crystallogr., Sect. B*, 1991, **47**, 192.